J. Cell. Mol. Med. Vol 15, No 2, 2011 pp. 396-413

Glomerular parietal epithelial cells of adult murine kidney undergo EMT to generate cells with traits of renal progenitors

Swetha G., Vikash Chandra, Smruti Phadnis, Ramesh Bhonde *

Tissue Engineering and Banking Laboratory, National Centre for Cell Science, Pune, India

Received: May 7, 2009; Accepted: October 5, 2009

Abstract

Glomerular parietal epithelial cells (GPECs) are known to revert to embryonic phenotype in response to renal injury. However, the mechanism of de-differentiation in GPECs and the underlying cellular processes are not fully understood. In the present study, we show that cultured GPECs of adult murine kidney undergo epithelial–mesenchymal transition (EMT) to generate cells, which express CD24, CD44 and CD29 surface antigens. Characterization by qRT-PCR and immunostaining of these clonogenic cells demonstrate that they exhibit metastable phenotype with co-expression of both epithelial (cytokeratin-18) and mesenchymal (vimentin) markers. Transcript analysis by qRT-PCR revealed high expression of metanephric mesenchymal (Pax-2, WT-1, Six-1, Eya-1, GDNF) and uteric bud (Hoxb-7, C-Ret) genes in these cells, indicating their bipotent progenitor status. Incubation of GPECs with EMT blocker Prostaglandin E2, resulted in low expression of renal progenitor markers reflecting the correlation between EMT and acquired stemness in these cells. Additional *in vitro* renal commitment assays confirmed their functional staminality. When injected into E13.5 kidney rudiments, the cells incorporated into the developing kidney primordia and co-culture with E13.5 spinal cord resulted in branching and tubulogenesis in these cells. When implanted under renal capsule of unilaterally nephrectomized mice, these cells differentiated into immature glomeruli and vascular ducts. Our study demonstrates that EMT plays a major role in imparting plasticity to terminally differentiated GPECs by producing metastable cells with traits of kidney progenitors. The present study would improve our understanding on epithelial cell plasticity, furthering our knowledge of its role in renal repair and regeneration.

Keywords: glomerular parietal epithelial cells • EMT • stem cell phenotype • renal progenitors • metastable cells

Introduction

Kidney is an organ with limited turnover of cells but exhibits remarkable ability to survive injury and restore function [1]. The precise mechanism by which adult kidney replenishes damaged cells remains to be understood. It is still not clear whether cellular repair in adult kidney is carried out by specialized renal progenitors residing in specific niches or by self-duplication/de-differentiation of mature cells. Previous reports suggest the role of renal resident stem cells in kidney repair and regeneration [2–5] and others have suggested the contribution of circulating bone marrow stem cells in renal repair [6]. However, limited contribution of these cells to injured kidneys has led to questions regarding their significance in kidney repair [7]. In vital organs like kidney, with low cell turnover it would be imperative to consider that organ repair would follow a more pragmatic way, wherein somatic cells would acquire phenotypic flexibility rather than activating the quiescent resident stem cell population [8]. It is well established that kidney tubular epithelial cells, respond to injury by de-differentiating into mesenchymal phenotype thus recapitulating the processes active during early nephrogenesis [9]. Furthermore, a recent report suggests that regeneration by surviving tubular epithelial cells is the predominant mechanism of repair in ischemic kidneys [10]. Interestingly, the response of glomerular cells to injury is reported to be more complex, involving considerable phenotypic adaptations [11]. Glomerular parietal epithelial cells (GPECs), lining the inner aspect of Bowman's capsule is known to respond to injury by de-differentiating into embryonic phenotype, similar to that of myofibroblasts with *de novo* expression of α-SMA [12]. Under normal physiological conditions, GPECs are known to migrate and differentiate into glomerular podocytes [13]. Moreover, reports suggest that $CD133^+$ $CD24^+$ cell subset of GPEC of adult human kidney have stem cell properties and participates in renal repair [14]. Reparative responses in differentiated glomerular epithelial cells thus repre-

*Correspondence to: Ramesh BHONDE,
Tissue Engineering & Banking Laboratory,
National Centre for Cell Science, NCCS Complex,
Ganeshkhind, Pune 411 007, Maharashtra, India.
Tel.: +91-20-25708079
Fax: +91-20-25692259
E-mail: rrbhonde@gmail.com

doi:10.1111/j.1582-4934.2009.00937.x

sent an injury-dependent regression from adult phenotype to embryonic mesenchymal phenotype [15]. It is suggested that such phenotypic alterations are primarily conceived by glomerular epithelial–mesenchymal trans-differentiation (GEMT) [16]. However, in certain conditions, these changes are also associated with excessive production of extracellular matrix (ECM) resulting in crescent formation and irreversible renal fibrosis [17]. It is intriguing that renal pathology is caught in this vicious cycle where normal patho-physiological responses to tissue injury such as EMT and fibrosis, can also result in chronic injury culminating in organ failure. Understanding the mechanism of cellular de-differentiation in key glomerular subsets like GPECs would further our knowledge of its role in tissue repair, disease progression and enable more effective targeted therapies for acute and chronic kidney diseases. With this perspective, we investigated the de-differentiation potential of murine glomerular epithelial cells, *in vitro*. We report here that GPECs of adult murine kidney undergo spontaneous EMT to generate cells with metastable phenotype and acquire gene profile and functional properties similar to that of early renal progenitors.

Materials and methods

Animals

Swiss Albino mice (6–8 weeks old) obtained from Jackson laboratories (Bar Harbor, ME, USA) were used for the study. The animals were maintained at the experimental animal facility of National Centre for Cell Science and experimental procedures performed according to institutional ethical guidelines. For isolation of kidney tissue, animals were killed by cervical dislocation and kidneys collected in sterile phosphate buffer saline (PBS). For isolation of E13.5 kidney and spinal cord, breeding pairs were set and pregnancy was confirmed by observing vaginal plugs. Pregnant females were killed at defined interval and kidneys and spinal cord dissected out.

Glomerular parietal epithelial cell culture

GPEC culture was done as previously described [14]. Briefly, kidneys of adult Swiss-Albino mice were washed and perfused with sterile PBS. The tissue was dissected into pieces, washed with sterile PBS, cut into smaller fragments and subsequently digested with collagenase-type-1(Sigma-Aldrich, St. Louis, MO, USA) [0.1 mg/ml in Hank's balanced salt solution (HBSS)] for 10 min. at 37°C. The enzymatic digestion was kept minimum so that Bowman's capsule is not digested and the yield of capsulated glomeruli is high. Gross remnants after collagenase digestion were allowed to settle for 1 min. and supernatant transferred to a new tube with complete medium and centrifuged at 400 × *g* for 3 min. Pellet containing glomeruli were sieved and plated into 60 mm culture dishes in Roswell Park Memorial Institute (RPMI) medium with 20% fetal calf serum (FCS) (GIBCO; Invitrogen). After 5–7 days glomerular explants with epithelial cell outgrowth were picked using clonal rings and cultured separately in 24-well plates. Cells were maintained in RPMI with 10% FCS and routinely passaged. For EMT blocking experiments, GPECs were cultured in RPMI with 10% FCS supplemented with 0.1 μM Prostaglandin E2 (Sigma-Aldrich). Media were changed every day.

Immunostaining and confocal microscopy

Cells on cover slips, cryostat sections and whole mount tissues were fixed in 4% fresh paraformaldehyde, permeabilized with 0.1% Triton-X100 and blocked with 1% bovine serum albumin (BSA). Primary antibodies were incubated overnight at 4°C, washed with PBS and then incubated with secondary antibody at 37°C for 1 hr. DAPI (4′, 6-diamidoino-2-phenylindole)/Hoechst 3342 (Invitrogen, Carlsbad, CA, USA) were used to visualize nuclei. Cells were washed with PBS and mounted on slides with Vectashield (Vector Laboratories, Burlingame, CA, USA). Confocal images were captured using Zeiss LSM 510 laser scanning microscope using 63×/1.3 /100× oil objective. Magnification, laser and detector gains were set below saturation. Images were analysed with LSM5 IMAGE EXAMINER software (Carl Zeiss, MicroImaging, Inc., Thornwood, NY, USA). The fluorescence is quantified and represented in 2.5D intensity graphs [18]. Results presented are representative fields confirmed from at least three different experiments. The sources of antibodies and dilutions used are summarized in Table 1.

Flow cytometry

Cells were trypsinized, centrifuged and blocked in 1% BSA. For the detection of surface antigens, cells were incubated with freshly diluted fluorescein isothiocyanate (FITC)/phycoerythrin (PE) conjugated antibodies for 1 hr at 37°C. The sources of antibodies and dilutions used are summarized in Table 1. Cells were also stained with FITC- or PE-labelled isotype-matched immunoglobins, which served as negative controls. Cells were washed with PBS, passed through 40 μm cell stainer to avoid clumps and resuspended in Fluorescence Activated Cell Sorting (FACS) buffer. The cells were analysed using BD FACSCanto™ Flow Cytometer and data quantified using BDFACS Diva softwarev5.0. For clonogenic studies, cells labelled with CD24 antibody were sorted as positive and negative fractions into individual wells of a 96-well plate at a density of one cell per well per plate for each fraction using BD FACSAria™ Flow Cytometer in sterile conditions. Wells with single cells were marked and confirmed under phase contrast microscope and maintained in standard culture conditions for colony formation.

RNA isolation and quantitative real time PCR

Tissue/Cells samples were frozen in Tri Reagent (Sigma-Aldrich). Total RNA was isolated from samples as per the manufacturers' instructions, measured on ND-100 spectrophotometer (Nanodrop Technologies, Wilmington, DE, USA). Two micrograms of RNA was used for cDNA synthesis per 20 μl reaction. cDNA was amplified using Reverse Transcription System Kit (ImProm II Reverse Transcription system #A3800, Promega Corporation, Madison, WI, USA). The primer sequences used for quantitative real-time polymerase chain reaction (qRT-PCR) are summarized in Table 1. qRT-PCR was performed in duplicate of total 25 μl reaction mixture containing 1× *Power* SYBR-Green Master-mix (Applied-Biosystems, Foster City, CA, USA), 600–750 nM each forward and reverse primers using 1/20th of the cDNA preparation. PCR amplification was carried out using Applied-Biosystem7300 Real-Time PCR Sequence detection System (SDS-v1 3.1; Applied-Biosystems).Cycling conditions were set as (program: 2 min. at 50°C, 10 min. at 95°C, and 35 cycles of 15 sec. at 95°C and 1 min. at 60°C). All qRT-PCR results were normalized to glyceraldehyde-3-phosphate-dehydrogenase (GAPDH) carried out in duplex reaction to correct differences in RNA input. Gene expression is reported as fold difference in C_T values relative to the expression of gene in cells at P5 over P1. Gene expres-

Table 1 The list of Primers and Antibodies with dilutions used in the present study

	Antibody	Company	Dilution
1	α smooth muscle actin	Sigma, www.sigma-aldrich.com	1–100
2	Aquaporin-6	(Chemicon) Millipore, www.millipore.com	1–100
3	β-Catenin	Sigma, www.sigma-aldrich.com	1–100
4	Cadherin-11	Millipore, www.millipore.com	1–100
5	Collagen II	Millipore, www.millipore.com	1–100
6	Collagen IV	Sigma, www.sigma-aldrich.com	1–100
7	Cytokeratin-18	Sigma, www.sigma-aldrich.com	1–100
8	E-Cadherin	Sigma, www.sigma-aldrich.com	1–100
10	Fibronectin	Millipore, www.millipore.com	1–100
11	Ki-67	Millipore, www.millipore.com	1–150
12	Laminin	Sigma, www.sigma-aldrich.com	1–100
13	Nephrin	Santa Cruz www.scbt.com	1–100
14	Nestin	Millipore, www.millipore.com	1–100
15	PECAM	Sigma, www.sigma-aldrich.com	1–100
16	Vimentin	Sigma, www.sigma-aldrich.com	1–100
17	Claudin1	Santa Cruz www.scbt.com	1:75
18	Claudin1/2	Santa Cruz www.scbt.com	1:75
17	CD29-FITC	BD, www.bdbiosciences.com	1–100
19	SCA-1-FITC	BD, www.bdbiosciences.com	1–100
20	CD24-FITC	BD, www.bdbiosciences.com	1–100
21	CD31-FITC	BD, www.bdbiosciences.com	1–100
22	CD11b	BD, www.bdbiosciences.com	1–100
23	CD105-PE	BD, www.bdbiosciences.com	1–100
24	CD45-PE	BD, www.bdbiosciences.com	1–100
25	CD38-PE	BD, www.bdbiosciences.com	1–100
26	CD90.1-PE	BD, www.bdbiosciences.com	1–100
27	CD44-PE	BD, www.bdbiosciences.com	1–100
28	C-KIT-PE	BD, www.bdbiosciences.com	1–100
29	CD88-PE	BD, www.bdbiosciences.com	1–100
30	CD133	Santa Cruz www.scbt.com	1–100

Continued

Genes		Primer sequence
WNT4	F	GCA GAT GTG CAA ACG GAA CCT TGA
	R	ATG TGG CTT GAA CTG TGC ATT CCG
WNT7b	F	AAC TTG CTG GAC CAC GCT ACC TAA
	R	TTG CAC TTG ACG AAG CAA CAC CAG
WNT9b	F	TGC CAC CTT GTC TCC TTG TCT TGA
	R	ATC TCT TCC AGG CAT TTG GAC CCT
WNT11	F	TGC CTC CCT GGA AAC GAA GTG TAA
	R	TGT CAC TGC CGT TGG AAG TCT TGT
WNT2b	F	CAA ATT CCA CTG GTG CTG TGC TGT
	R	AGG CAG AGT AGC ATC AAA CAC GGA
WNT6	F	TGT CAG TTC CAG TTC CGT TTC CGA
	R	GCT TGT GCT GCG CAT CCA TAA AGA
WNT5b	F	TGG AAA TCC ACA ACC AGT GGG AGA
	R	AGC AGG TGA CAG AAC CGT CTT TCT
TGF-β_1	F	TAA AGA GGT CAC CCG CGT GCT AAT
	R	AAA GAC AGC CAC TCA GGC GTA TCA
TGF-β_2	F	AAG GCG TTA GTC TGC ATC TCA CCT
	R	AAT CAT GCT GGC TTC TAG ACC CGT
TGF-β_3	F	CAG GGC AAG GCA AAG AGC TTG ATT
	R	TAT CTG ATA TCG CCC AAC GCT GCT
BMP-7	F	GAA AAC AGC AGC AGT GAC CA
	R	GGT GGC GTT CAT GTA GGA GT
Pax-2	F	TCC CAG TGT CTC ATC CAT CA
	R	GTT AGA GGC GCT GGA AAC AG
WT-1	F	TAC AGA TGC ATA GCC GGA AGC ACA
	R	TCA CAC CTG TGT GTC TCC TTT GGT
Eya-1	F	AGC AGC TTT ACC ACG TCA TCA GGA
	R	ATG GGT GTG GAA GGA CTG TGG ATT
Six-1	F	ACC ACT GTT TCT TCT CCA CAG CCT
	R	TAC AAA GCA TGA GCA AGC CAA CCC
Odd 1	F	AGA GTG TGG GAA AGG ATT CTG CCA
	R	TGC TGT GGA AGG AAG ATC CCG AAA
K-Cadherin	F	AGG AGG AAT GAG CCT GGA TTT GGT
	R	TTC CTC TTT GCT GGG AAG CCA CTA
GDNF	F	AAA GCA TTC CGC TAA ACG GTG TGG
	R	TTT CTG TAG CTG GGC CTT CTT CCA

Continued

Table 1 Continued

Genes		Primer sequence
Hox b7	F	AGA AAG CCA AGA GGA GGA AAG CGA
	R	GGC ACA TTC CAG AAA GCC ACA GAA
C-Ret	F	ACG ATG ACA CAG GAG AAG CGG ATT
	R	TAG CAC TGG CTT CGT GAG TGA CAA
Vimentin	F	ATG CTT CTC TGG CAC GTC TT
	R	AGC CAC GCT TTC ATA CTG CT
Nestin	F	ATA CAG GAC TCT GCT GGA GG
	R	AGG ACA CCA GTA GAA CTG GG
Cytokeratin19	F	AGT TTG AGA CAG AAC ACG CCT TGC
	R	TCA GGC TCT CAA TCT GCA TCT CCA
E-Cadherin	F	TGA CTC GAA ATG ATG TGG CTC CCA
	R	ACT GCC CTC GTA ATC GAA CAC CAA
Claudin 3	F	TGA CAG ACG ACA CAC AGT CTG CTT
	R	TCC ATT CGG CTT GGA CAG TTC CTA
Claudin 4	F	ATG GTC ATC AGC ATC ATC GTG GGT
	R	TGT AGA AGT CGC GGA TGA CGT TGT
Occludin	F	AGC AGC CCT CAG GTG ACT GTT ATT
	R	ACG ACG TTA ACT CCT GAA CCA GCA
Snail 1	F	ACA GCT GCT TCG AGC CAT AGA ACT
	R	TGT ACC TCA AAG AAG GTG GCC TGA
Snail 2	F	CAC ATT CGA ACC CAC ACA TTG CCT
	R	TGT GCC CTC AGG TTT GAT CTG TCT

sion analysis for PGE2 treated cells is represented as fold difference in C_T values relative to expression of the genes in untreated cells at P1 and P5.

Microinjection of CD24$^+$ cells to E13.5 kidney

The cells were trypsinized and stained with fluorescent cell marker chloromethylfluorescein diacetate (CMFDA) (Invitrogen) as per manufacturer's instruction. Briefly, cells were incubated with 5 μM of CMFDA dye at 37°C for 30 min. in plain medium. The cells were then washed and incubated in normal culture medium. Fluorescent labelled cells were then resuspended in 20 μl of PBS to make a final concentration of 10^6 cells/ml and microinjected with a very fine needle into E13.5 embryonic kidneys on a transwell membrane. E13.5 kidneys were cultured in air media interface in normal culture media for 3–5 days.

Co-culture of CD24$^+$ cells with E13.5 spinal cord

For *in vitro* induction experiments, cells were co-cultured with E13.5 spinal cord using cell culture inserts in serum-free media [(RPMI1640 with 1% BSA and 0.25 μl beta-mercaptoethanol (BME)]. Cells were seeded in 6-well plates and insert containing spinal cord were slowly lowered. Media were changed every 24 hrs and conditioned media collected. After 5 days in culture, to promote tubulogenic differentiation, the embryoid bodies (EBs; nephrospheres) formed were transferred to matrigel coated plates and cultured for additional 5 days in E13.5 spinal cord conditioned media.

In vitro tube formation assay

For endothelial differentiation, 2×10^5 cells were seeded onto Matrigel (250 μl) (BD Biosciences, San Diego, CA, USA) coated 24-well plates in normal culture media. The cells were incubated in 37°C, 5% CO_2 and observed for 24 hrs. Cells were then separated from the matrigel by 1 hr/37°Cincubation with Dispase (1 mg/ml). Isolated cells were then analysed by flow cytometry for the expression of endothelial specific markers.

Unilateral nephrectomy in mice

Unilateral nephrectomy was performed on 6–8-week-old Swiss albino mice as described earlier [19]. Under anaesthesia (ketamine [150 mg/kg] and xylazine [10 mg/kg]), right kidney was exposed through a small lumbar incision. The renal artery was ligated and the kidney excised. The right kidney was removed in all experimental groups ($n = 10$). The animals were kept warm during and after the procedure, using a heating lamp. Incisions were closed using 4–0 absorbable sutures. Animals returned to cages and were kept in postoperative care with adequate food and water.

Cell implantation under kidney capsule

Before implantation under kidney capsule, the cells were labelled with fluorescent dye PKH26 (Red Fluorescent Cell linker Kit, Sigma-Aldrich) as per manufacturer's instructions. Briefly, 4 μM of PKH26 cell linker dye was incubated with 2×10^6 cells. Cells were washed separately with PBS and staining was stopped by adding complete media with FCS. The cell implantation was carried out following the protocol described earlier [20]. Briefly, under anaesthesia, the labelled cell suspensions were mixed with equal volume of mouse autologous tail vein blood and the resulting clot was then implanted under the kidney capsule. Use of blood clot helps in the localization of the grafts and prevents loss of cells. Implants were removed 2 weeks after nephrectomy of the contra-lateral kidney and processed for further analysis. For histological evaluation of the grafted cells, sections were stained with haematoxylin and eosin.

Statistical analysis

Values are expressed as mean ± S.E.M. from three different experiments unless otherwise indicated. Statistical analysis was done using paired two-tailed, t-test to determine the significance between different conditions. *P*-values < 0.05 were considered significant Prism4, Graphpad Software; (http://www.graphpad.com) was used for all analysis.

Results

Glomerular parietal epithelial cells of adult murine kidney generate CD24$^+$ mesenchymal cells *in vitro*

Capsulated glomerular explants derived from collagenase digested murine kidney gave rise to a number of epithelioid colonies *in vitro* (Fig. 1A). The epithelial nature of these cells was established by their polygonal shape and cobblestone appearance at confluence. The parietal epithelial nature of these cells was established by positive immunostaining for Claudin-1 and 2 [21], also co-expressing CD24 (Fig. 1B). GPECs were positive for E-Cadherin and CD24 (Fig. 1C) but negative for podocyte marker, nephrin (Fig. 1D) and endothelial marker, Von-Willibrand factor (VWF) (Fig.1E). Immunostaining of normal murine kidney for the expression of CD24 showed that the antigen is localized in cells lining the Bowman's capsule and certain cells of proximal tubules (Fig. 1F). By 5–6 days in culture, epithelial outgrowths from individual glomeruli were isolated by ring cloning and cultured in 24-well plates. Under *in vitro* conditions, the typical cobblestone pattern of the cultured epithelial cells was gradually (7–8 days) replaced by spindle-shaped fibroblast-like cells. After the cells were expanded to sufficient numbers for cloning they were sorted to CD44$^+$ and CD24$^+$ dual positive cells and designated as passage1(P1). At P1, 99.7 $\pm$ 0.3% cells were dual positive for CD44 and CD24 antigens and further characterization showed that these cells exhibited uniform expression for CD44 (94 $\pm$ 3.1%) and CD29 (99 $\pm$ 0.25%) A detailed CD marker analysis showed that the cells were negative for CD133 and other lineage specific markers (CD45, CD11b, CD38, etc.) (Fig. 2A). All clones from GPEC ($n = 6$) consistently exhibited this surface antigen profile throughout passages. However, in certain clones ($n = 2$), we observed intermittent fluctuation with respect to CD24 antigen (Fig. 2B). Single cell cloning of CD24$^+$ and CD24$^-$ fractions and subsequent analysis of the colonies revealed that the antigenic flux is not due to co-existence of independent cell populations since culturing of isolated CD24$^+$ and CD24$^-$ fractions restored cells with original expression profile (Fig. 2C).

Metastable mesenchymal cells are generated *in vitro* through EMT

The phenotypic shift in parietal epithelial cells to CD24$^+$ mesenchymal cells indicated that EMT may be operational in these cells under *in vitro* culture conditions. Transcript analysis of CD24$^+$ cells at P5 as compared to that of P1, for epithelial and mesenchymal genes confirmed that these cells have undergone EMT. Quantitative real time PCR performed on the sorted cell fractions showed significant down-regulation of the epithelial genes, E-Cadherin, Occludin, Cytokeratin-19), Claudin-3, claudin-4 and a simultaneous up-regulation of mesenchymal genes, vimentin and nestin in CD24$^+$ cells from P-1 to P-5. The down-regulation of cell adhesion molecules was concomitant with the high expression of major regulators of EMT, Snail-1 and Snail-2. Further, we examined the level of common initiators of EMT, which include members of transforming growth factor (TGF)-β family of genes in these cells. Transcript level of TGF-β_1 gene, the key EMT modulator, was high in CD24$^+$ cells at P1 and maintained its expression throughout passages. Significant up-regulation in the expression of TGF-β_2 transcript and slight up-regulation of TGF-β_3 transcripts was observed in these cells. The up-regulation of TGF-β_1 transcript from P1 to P5 was followed by concurrent down-regulation of BMP-7(Fig. 3A), which is known to counteract TGF-β_1 induced EMT [22].

Sequestration of E-Cadherin from the cell surface in P-1 to the perinuclear vesicles in P-5 of these cells (Fig. 3B) reinforced the occurrence of EMT like changes in these cells. The enriched CD24$^+$ cells showed positive staining for mesenchymal proteins nestin, fibronectin, α smooth muscle actin and collagen-I (Fig. 3C). Co-expression of epithelial and mesenchymal transcripts in the CD24$^+$ clonal cells indicated metastable phenotype of these cells. To clarify that individual cells in CD24$^+$ colony express both epithelial and mesenchymal markers and not that a sub-population of these cells are becoming mesenchymal regardless of the CD24 status, we carried out clonogenic assay ($n = 5$) for cells at P1 and P5. The colonies were probed for the co-expression of the mesenchymal protein, vimentin and epithelial marker cytokeratin-18. Our data indicate that at P1, the cells express high abundance of CK-18 but low levels of vimentin which was localized in the nuclei. By P5, vimentin expression was up-regulated along with CK-18 (Fig. 3D) suggesting that EMT rendered metastable phenotype to these cells.

CD24$^+$ metastable cells generated through EMT intrinsically express markers of early kidney progenitors

Studies have shown that the process of EMT renders stem cell like characteristic to cells during embryonic development [23]. To examine whether CD24$^+$ cells demonstrate any such progenitor profiles, we checked for the co-expression of Cadherin 11 with CD24, surface markers of renal progenitors [24]. We found that 94.7 $\pm$ 2.1% of these cells showed co-expression of CD24 and Cadherin-11 (Fig. 4A) indicating that these cells have acquired stem cell like properties. These cells also exhibited high expression of CXCR4 (78.7 $\pm$ 2.3%), the chemokine required for homing and regenerative potential of renal progenitors [25] (Fig. 4B). Data obtained from qRT-PCR analysis ($n = 3$) of CD24$^+$ cells at P1 for kidney progenitor markers, revealed transcript abundance of Pax-2, WT1, GDNF, Eya-1, Six-1 and Odd1, which are a set of pivotal genes involved in mammalian kidney development [26]. As EMT progressed from P1 to P5, significant up-regulation in the expression of major progenitor makers (Eya-1, Six-1 Odd1, WT-1 and GDNF) was observed. No change in transcript abundance was

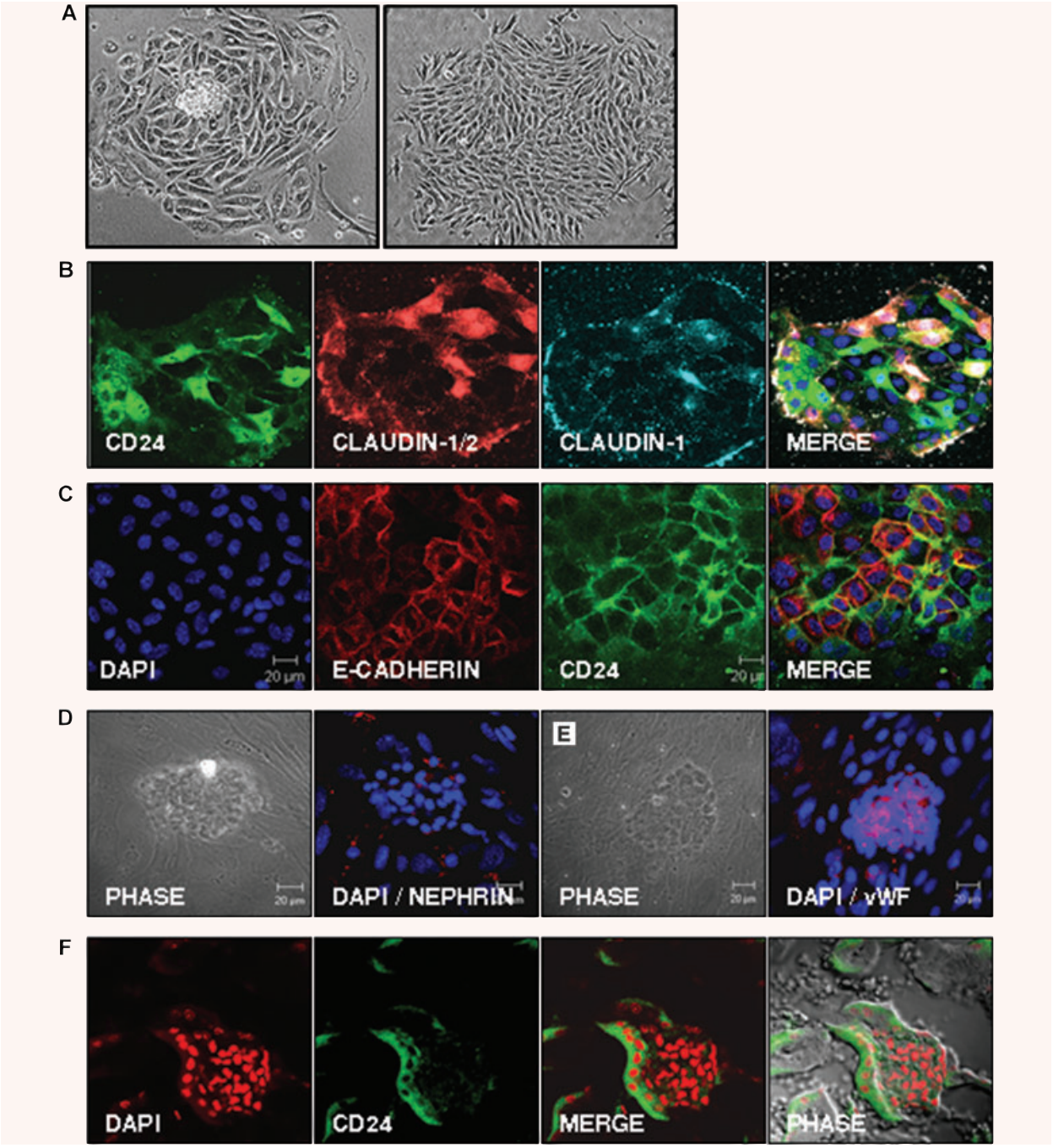

Fig. 1 Generation and characterization of GPECs. Capsulated glomeruli isolated from collagenase digested adult murine kidney were plated on culture dishes ($n = 6$). By day 7, compact cell bodies were abundant, surrounding the parent glomeruli, *in vitro* culture of GPECs led to loss in epithelial phenotype and resulted in clonogenic cells with mesenchymal phenotype (**A**). Primary GPECs showed CD24 (green) immunostaining which co-expressed with Claudin-1/2 (red) and claudin-1(cyan) (**B**). The cells exhibited tight intercellular junctions; confocal images showing E-Cadherin (red) and CD24 (green) co-expression in these cells (**C**), Nuclei stained with DAPI. Lack of nephrin (**D**) and VWF (**E**) expression in the cellular outgrowth ruled out the possibility of podocytes or endothelial cells in culture. Cryosections of mouse kidney showing CD24 (green) localization in cells lining the Bowman's capsule, nuclei are stained by DAPI, represented in red (**F**). Results are representatives of at least three independent experiments. Abbreviations: VWF – Von-Willibrand factor, DAPI-4′, 6-diamidoino-2-phenylindole.

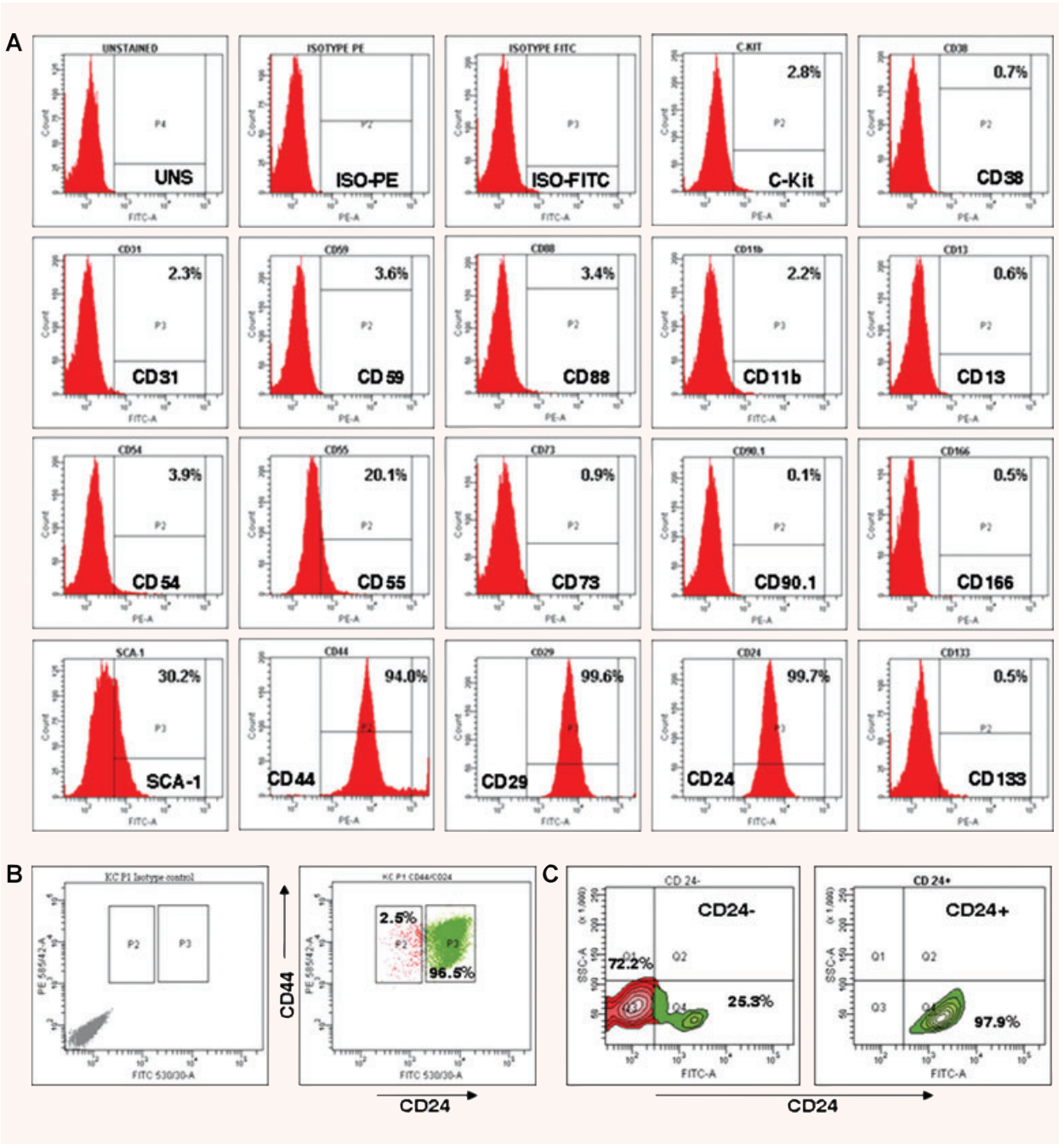

Fig. 2 Immunophenotypic profile of the flow sorted CD44$^+$ CD24$^+$ cells. Flow cytometry histograms show the expression of selected CD markers (CD44, CD29, CD24 and SCA-1 (low intensity) and no expression of other mesenchymal/lineage specific markers (CD31, CD11b, CD133, CD105, CD90.1, etc.) (**A**). CD24$^+$ cells undergo antigenic flux *in vitro*. Cells show homogenous expression of CD44 but show distinct variation in the expression of CD24 (**B**), isotype control is shown. Analysis of single cell clones of CD24$^-$ and CD24$^+$ cells for CD24 expression. CD24$^-$ and CD24$^+$ Cells were singly sorted into 96-well plates, 10–13 wells showed presence of single cells which were further expanded and analysed. Follow-up studies show that the CD24$^-$ population after two population doublings reverts to the CD24$^+$ profile (**C**).

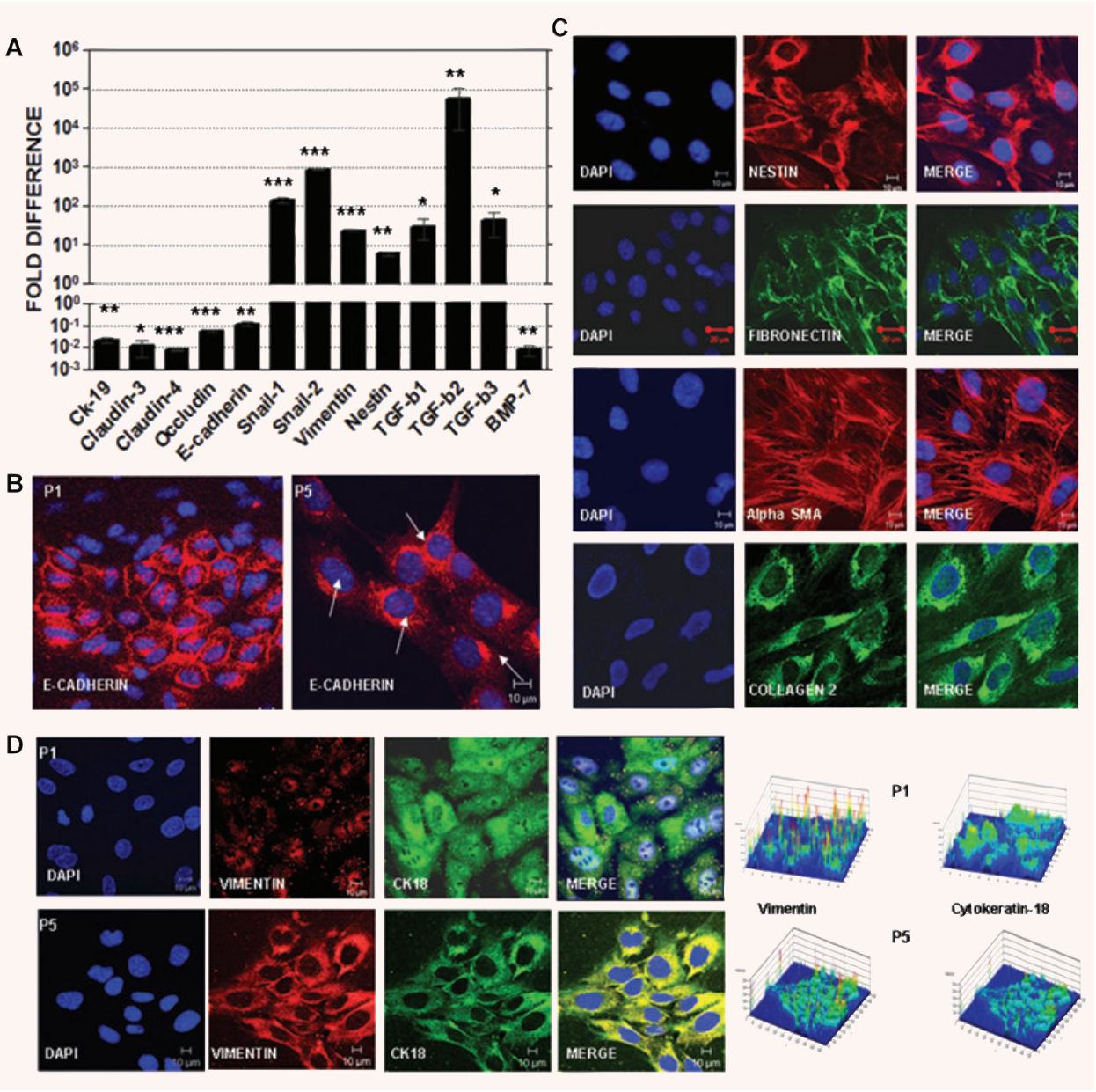

Fig. 3 GPECs undergo epithelial EMT *in vitro*. qRT-PCR analysis for the expression of epithelial and mesenchymal markers as well as transcript levels of major EMT regulators in $CD24^+$ cells at passage 5 over P1($n = 3$). Graphs are represented as fold difference in Ct value of passage 5 over passage 1. RNA was obtained from single cell colony of $CD24^+$ cells at passages 1 and 5. All mRNA expression levels were normalized to the house keeping gene GAPDH expression. Data are represented as mean ± S.E.M., ($^*P < 0.05$, $^{**}P < 0.01$, $^{***}P < 0.001$). Transcript abundance of the EMT specific genes is estimated by duplex quantitative real-time PCR for 35 cycles (**A**). Confocal image showing the sequestration of membrane bound E-Cadherin in cells at P1 to perinuclear space in cells at P5, nuclei stained with DAPI (**B**). Confocal fluorescent images showing the expression of mesenchymal cytoskeletal proteins in $CD24^+$ cells (P5) nestin, fibronectin, α-smooth muscle actin, collagen 2 (**C**). Clonogenic assay of the cells show co-expression of epithelial and mesenchymal marker, indicating metastable phenotype in these cells confocal image of a representative $CD24^+$ cell colony at P1show low expression of Vimentin (red) and high level of CK-18 (green). By passage 5, the cells exhibit uniform expression levels of vimentin (red) and CK-18 (green) (**D**). Fluorescence is quantified and represented in 2.5D intensity graphs. Nuclei stained with DAPI (scale bar = 10 μm). Abbreviations: qRT PCR, quantitative reverse transcription polymerase chain reaction; GAPDH, glyceraldehyde-3-phosphate-dehydrogenase.

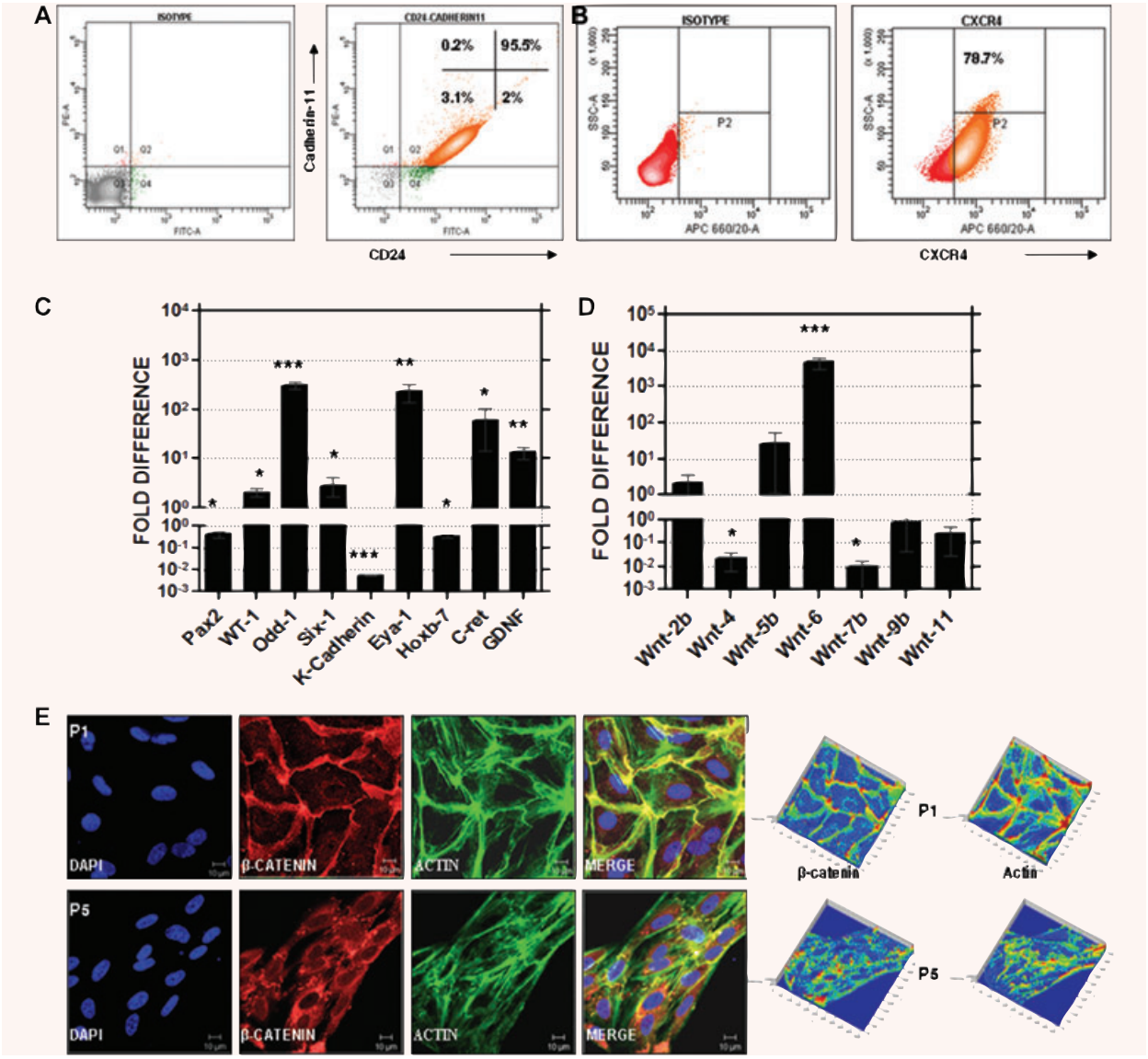

Fig. 4 CD24$^+$ cells express markers of embryonic renal progenitors. FACS analysis exhibits the co-expression of surface markers of embryonic renal progenitors in CD24$^+$ cells, CD24 and Cadherin-11(95.5 ± 2.1%), isotype control (**A**). The cells showed expression of CXCR-4 (78.7 ± 1.6%) (**B**). qRT-PCR was performed on CD24$^+$ cells for the expression of genes specific to metanephric progenitors ($n = 3$) (**C**). RNA was obtained from single cell colony of CD24$^+$ cells at passages 1 and 5. All mRNA expression levels were normalized to the house keeping gene GAPDH expression. Graphs are represented as fold difference in Ct value of passage 5 over passage 1. Data are represented as mean ± S.E.M. ($^*P < 0.05$, $^{**}P < 0.01$, $^{***}P < 0.001$). qRT-PCR analysis for Wnt gene expression of the cells at P5 over P1 ($n = 3$) (**D**). Confocal immunostaining of β-catenin localization in cells of P1 and P5. β-catenin translocated from the cell membrane at P1 to cytoplasm at P5. Fluorescence is quantified and represented in 2.5D intensity graphs. Scale bar represents 10 μm (**E**).

noted in case of Pax-2 and Hoxb-7. However, the expression of K-Cadherin was significantly down-regulated as EMT progressed from P1 to P5. Interestingly, we found that along with the markers of metanephric mesenchyme, CD24$^+$ cells consistently ($n = 3$) co-expressed markers of uteric bud (Hoxb-7 and C-Ret) suggesting a possible bi-potent progenitor status of these cells.

CD24$^+$ cells exhibit dynamic pattern of Wnt gene expression *in vitro*

During the reciprocal inductive mechanisms, active Wnt signalling is observed in the epithelial progenitors and metanephric

mesenchyme of the developing kidney [27]. To check if Wnt signalling is conserved in the $CD24^+$ cells similar to that in the early kidney progenitors; we studied the transcript profile of five canonical (Wnt-2b, Wnt-4, Wnt-6, Wnt-9b and Wnt-7b) and two additional Wnts (Wnt-5b, and Wnt-11) expressed in the embryonic kidney [28]. We found that all the Wnt genes studied are expressed in $CD24^+$ cells from P1 to P5, many of them in dynamic patterns. Wnt-4 is known to directly regulate E-Cadherin expression [29]. Corresponding to the down-regulation of E-Cadherin, we observed a down-regulation in the expression of Wnt-4 transcript from P1 to P5. Interestingly, the down-regulation of Wnt-4 also resulted in the up-regulation of Wnt-6, which is known to compensate for Wnt-4 in Wnt-4 null mice kidneys [28]. As EMT progressed from P1 to P5, we observed a concomitant reduction in the expression of Wnt-7b and Wnt-11b, which are stimulators of renal epithelial proliferation [30]. The Wnt-2b of metanephric mesenchyme Wnt-9b of uteric bud retained its expression throughout passages. Substantial increase in transcript abundance of Wnt-5b (expressed in the migratory mesenchymal cells) [31] was observed (Fig. 4D). Translocation of β-catenin from cell membrane (P1) to cell cytoplasm (P5), which is another hall mark event in EMT [32], was observed in these cells (Fig. 4E). However, no prominent nuclear β-catenin staining was observed.

Correlation between EMT and progenitor properties in GPECs

In order to confirm that EMT rendered traits of renal progenitors to GPECs, we carried out EMT blocking experiments with Prostaglandin-E2, a potent inhibitor of EMT [33]. The PEC outgrowth from renal glomeruli (P1) were treated with 0.1 μM PGE2 and cultured. We observed that PECs treated with PGE2 had lower proliferative potential and no apparent EMT like changes were observed in these cells. By 8–10 days, untreated cells proliferated and showed EMT like changes, (Ki-67 and nestin expression) (Fig. 5A.a) while no such changes were observed in GPECs treated with PGE2 (Fig. 5A.b). Further characterization by qRT-PCR revealed that incubation with PGE2 lowered cell proliferation (low expression of Ki-67 transcript) (Fig. 5B) and successfully inhibited EMT (low transcript abundance of mesenchymal markers) in these cells. GPECs treated with PGE2 had higher expression of all epithelial markers and low levels of mesenchymal markers when compared with untreated cells at P1 and P5 (Fig. 5C). Interestingly, we found that EMT blockage also resulted in low expression levels of most progenitor markers except epithelial markers K-Cadherin and Hoxb-7 whose levels were higher (Fig. 5D). Additionally, we observed that blocking EMT modulated Wnt gene expression pattern in these cells. Wnt genes associated with epithelial progenitors were up-regulated (Wnt7, Wnt9b and Wnt-11) over the mesenchymal Wnt genes (Wnt2d, Wnt-4, Wnt5b and Wnt6) whose transcript levels were low (Fig. 5E).

$CD24^+$ cells exhibit renal commitment *in vitro* as wells as *in vivo*

Encouraged by the transcript profile of the $CD24^+$ metastable mesenchymal cells, the functional renal commitment potential of these putative progenitors was assessed by *in vitro* and *in vivo* nephron development assays.

In vitro co-culture of $CD24^+$ cells with developing embryonic kidney (E13.5)

Here, we demonstrate the ability of $CD24^+$ cells to subsist, proliferate and integrate into the developing E13.5 kidney in an *in vitro* system. The $CD24^+$ cells (1000–1500 cells/tissue) tagged with green fluorescent dye marker CMFDA were injected into the kidney rudiments dissected from E13.5 kidney and cultured for 5 days on transwell filters without additional growth factors. Whole mount and antibody staining of the rudiments showed that the $CD24^+$ cells have integrated into the developing kidney. Optical sectioning of the whole mount kidney rudiment showed clusters of $CD24^+$ cells integrated with the 3D kidney primordia (Fig. 6A). Anti-laminin staining showed that the cells have integrated into the developing tubules and uteric-bud stalk [34] (Fig. 6B). PGE2 treated cells failed to integrate into the developing kidney. However, few cells remained attached to kidney surface (Fig. 6B).

In vitro co-culture of $CD24^+$ cells with E13.5 spinal cord

$CD24^+$ cells were co-cultured with E13.5 embryonic spinal cord, the heterologous inducer of metanephric mesenchyme and uteric bud [35]. After 2–3 days in culture, these cells aggregated to form EBs. Extended culture (5–6 days) of these EBs on matrigel in the presence of E13.5 spinal cord conditioned medium resulted in sprouting and network branching in more than 60% of cell aggregates ($n = 10$) (Fig. 6C). PGE2 treated cells on the other hand failed to form intact nephrospheres due to poor migration and no branching pattern were observed in these cells when grown on matrigel with E13.5 spinal cord conditioned medium(Fig. 6D).

$CD24^+$ cells exhibit endothelial differentiation potential *in vitro*

To analyse whether $CD24^+$ cells can differentiate into endothelial lineage and participate in angiogenesis, matrigel tube formation assay was carried out. A 16 hr culture on matrigel demonstrated the capillary formation ability of $CD24^+$ cells ($n = 6$) (Fig. 6D). The matrigel culture induced the expression of platelet endothelial cell adhesion molecule (PECAM) (CD31), an endothelial marker in ($92.2 \pm 6.5\%$) of these cells over undifferentiated cells (Fig. 6E).

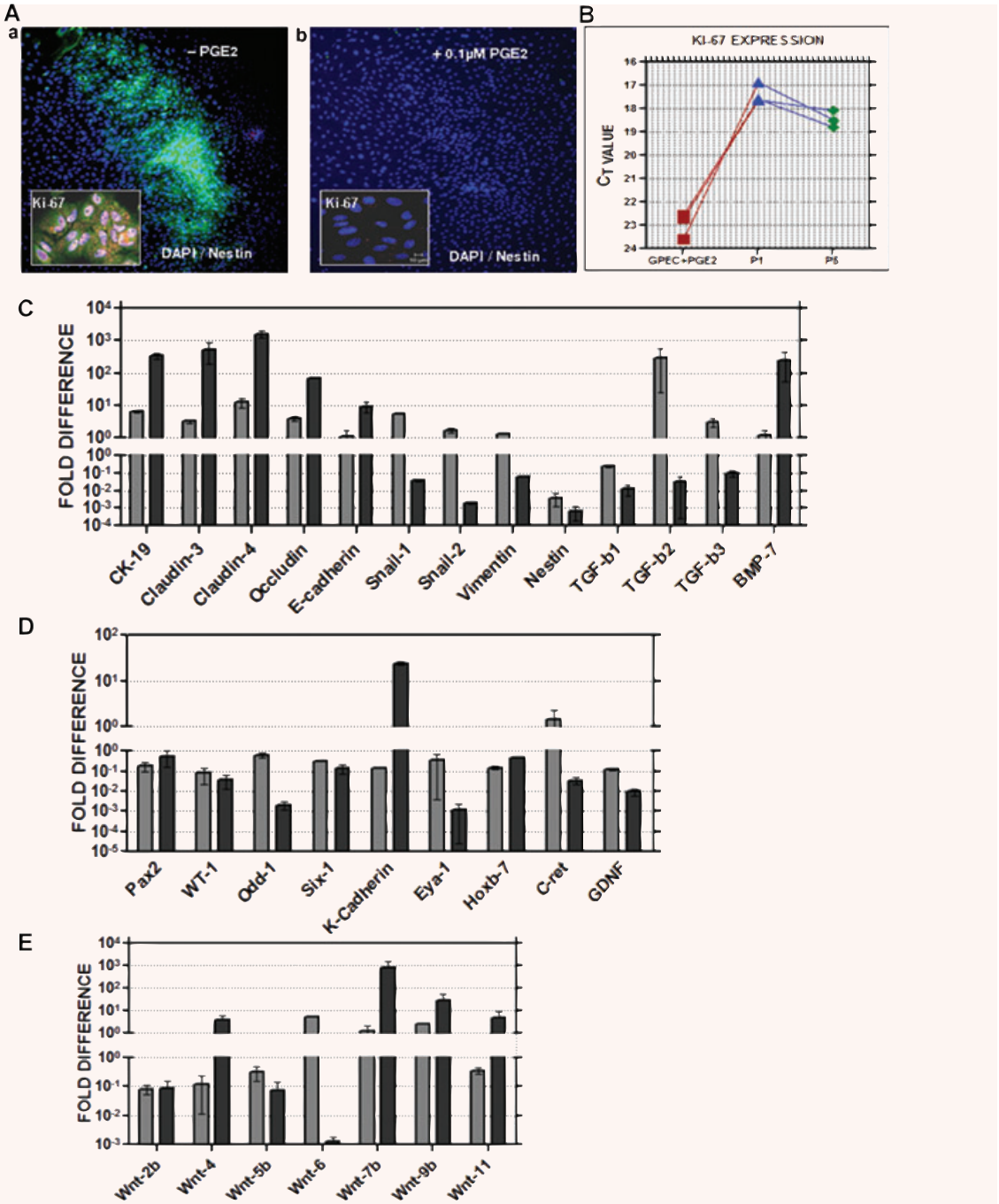

Fig. 5 EMT inhibition in GPECs by Prostaglandin E2. GPECs (P1) were incubated with 0.1 μM PGE2 and cultured for 2 weeks. Control GPECs without PGE2 treatment showed rapid proliferation, Ki-67 staining, inset and appearance of nestin positive cells within the colony (**A.a**) while cells incubated with PGE2 exhibited no nestin expression and low Ki-67 staining (**A.b**). qRT-PCR analysis showed that in cells incubated with PGE2, Ki-67 was highly down-regulated as compared to cells at P1 and P5 (**B**). qRT-PCR analysis of GPECs treated with PGE2 over cells at P1 and P5 for the expression of epithelial and mesenchymal markers as well as major EMT regulators (**C**). qRT-PCR analysis was carried out to compare the expression level of renal progenitor genes (**D**) and Wnt genes (**E**) in GPECs treated with PGE2 over untreated cells at P1 (grey bar) and P5 (black bar). Graphs are represented as fold difference in Ct value of cells treated with PGE2 over untreated cells at P1 and P5, Ct (PGE2-P1,) (PGE2-P5). All mRNA expression levels were normalized to the house keeping gene GAPDH expression. Data are represented as mean ± S.E.M. ($*P < 0.05$, $**P < 0.01$, $***P < 0.001$).

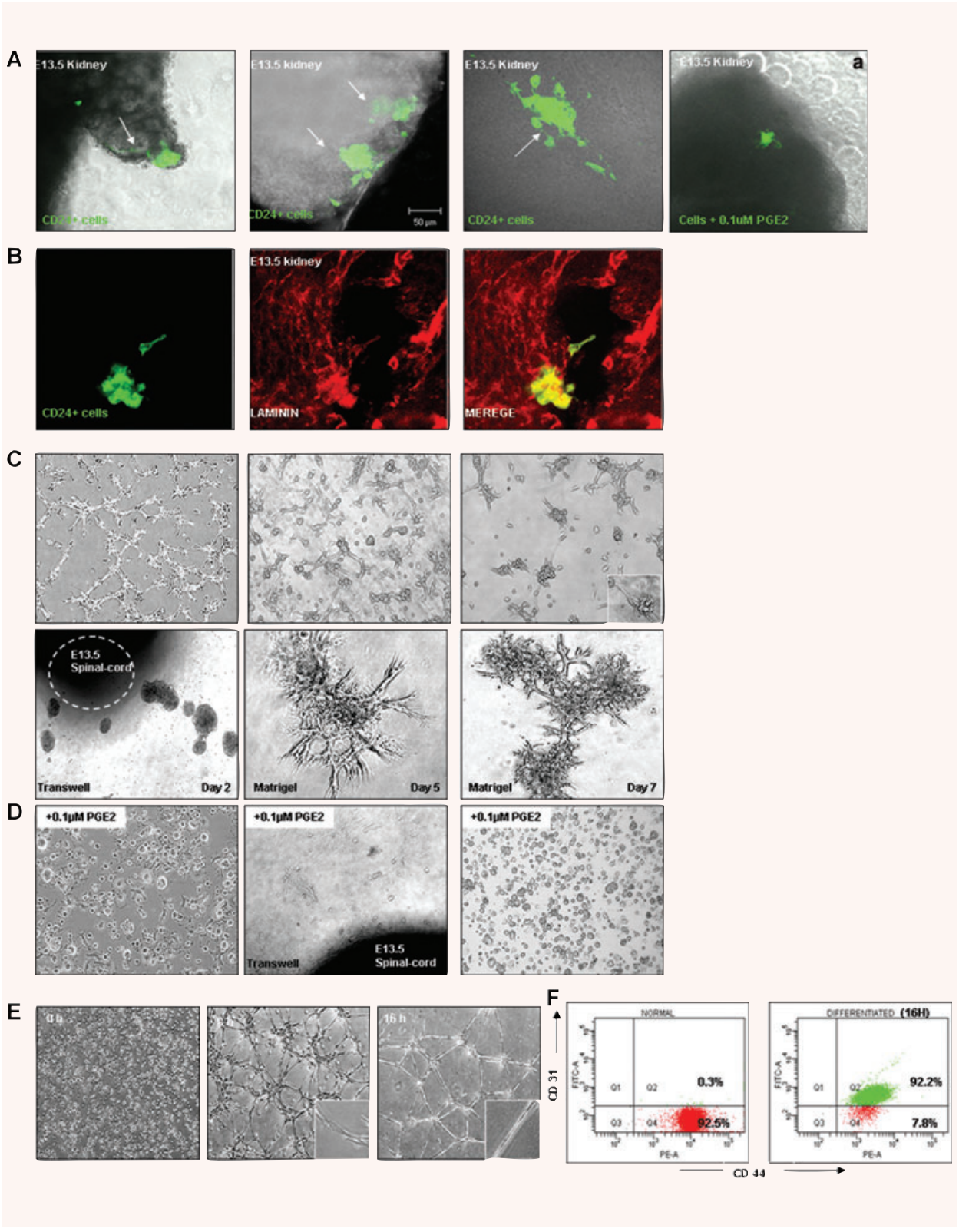

Fig. 6 *In vitro* renal commitment assays prove the functional progenitor status of $CD24^+$ cells. Nephron development assays were performed to assess the functional progenitor status of the cells. $CD24^+$ cells were fluorescently tagged with CMFDA and injected into E13.5 kidney cultured *in vitro* ($n = 6$). Whole mount staining of E13.5 kidney after 5 days of co-culture with cells (**A**). Note that cells treated with 0.1 μM PGE2 failed to integrate into the developing kidney (**A.a**). Confocal optical section of the whole mount staining of E13.5 kidney with cells for tubular protein laminin (**B**). Co-culture of cells with E13.5 spinal cord, heterologous inducer of uteric buds branching ($n = 6$). Cells were cultured for 5 days, placed next to embryonic E13.5 spinal cord on a transwell filter. Cells aggregated and formed EBs by d2 which was then cultured for an additional 5 days on matrigel in E13.5 conditioned media. Tubulogenesis and branching morphogenesis were observed in the EBs after 5 day in culture (**C**). Cells at P1 treated with PGE2 showed poor aggregation and survival potential in SFM. No branching or tubulogenesis was observed when grown on matrigel (**D**). Matrigel tube formation assay on $CD44^+$ $CD24^+$ cells ($n = 3$). A total of 2×10^5 cells were seeded on a layer of matrigel, cells started aligning in tandem by 8 hrs and tube formation was observed by 16 hrs on matrigel (**E**). Morphological changes of the cells were observed at various time-points under phase contrast microscope and photographed (100× magnification). Endothelial differentiation was confirmed by the expression of endothelial specific marker PECAM (CD31) (92.2 ± 6.5%) in the cells after differentiation over undifferentiated cells (0.3 ± 1%) (**F**). (Scale bar = 50 μm). Abbreviations: CMFDA, 5, chloromethylfluorescein diacetate; SFM, serum-free media; E-embryonic day; d, day; F, field; EB, embryoid body.

These results demonstrate that $CD24^+$ cells are capable of producing capillary structures *in vitro* by differentiating into endothelial cells.

$CD24^+$ cells exhibit *in vivo* differentiation potential when implanted under contra-lateral kidney capsule of unilaterally nephrectomized mice

Compensatory renal growth after unilateral nephrectomy is a remarkable regenerative mechanism exhibited by the kidney. After unilateral nephrectomy, the remaining kidney increases in size, the phenomenon is known as compensatory hypertrophy [19]. We reasoned that the mechanism of compensatory hypertrophy would provide an ideal growth and differentiation milieu for the putative kidney progenitors to exhibit renal commitment *in vivo* if any. FACS purified and PKH26 labelled cells (2×10^6 cells) were grafted under the left kidney capsule of normal mice ($n = 5$). One-week after implantation, unilateral nephrectomy of the right kidney was performed. Two weeks after nephrectomy mice were killed to visualize the status of the graft. The recovered grafts exhibited increase in size, were vascularized and no neoplasia were observed (Fig. 7A–D). Grafted $CD24^+$ cells generated neo-glomerular, vascular and ductal structures at 3 weeks after engraftment, as determined by histological assessment of fixed sections (Fig. 7E.a–e). The cryostat sections of $CD24^+$ graft showed that grafted cells underwent endothelial differentiation as demonstrated by the co-expression of PKH26 with PECAM in immature glomerular structures and vascular ducts (Fig. 8A). Co-expression of PKH-26 with surface localization of E-Cadherin confirmed epithelialization of the grafted cells (Fig. 8B). Flow cytometry analysis showed that 63.18 ± 5% PKH^+ cells were E-$Cadherin^+$ positive (Fig. 8C). Additional immunostaining of the grafted cells showed acquired expression of collagen 4 and laminin 1 (Fig. 9A, B) which are glomerular basement membrane components of immature nephron (comma and s-shape) [36] over cultured $CD24^+$ cells. Expression of intercellular vesicle water channel protein, Aquaporin-6 [37] and expression of mature podocyte marker nephrin was observed within the cells of the graft (Fig. 9C, D). The *in vivo* proliferation potential of the grafted cells was determined by Ki-67 staining (Fig. 9E). Grafting of $CD24^+$ cells in the renal capsule of normal (un-nephrectomized) mice produced no visible differentiation within the stipulated time (data not shown).

Discussion

In this study, we demonstrate that GPECs of adult murine kidney undergo spontaneous EMT *in vitro* to generate cells with characteristics and functional properties of embryonic renal progenitors. More importantly, by clonal assays we demonstrate that these cells adopt metastable phenotype, with attributes of both epithelial and mesenchymal markers. This suggests that parietal epithelial cells of the glomeruli act as potential stem cells and EMT could increase this ability. Earlier reports have shown the isolation of $CD24^+$ $CD133^+$ renal stem cells from PEC of human kidney [14]. In our study, GPECs were strongly positive for murine CD24 antigen but the cells did not show any expression for CD133. We speculate that this disparity may be due to species variability. An important aspect of our study is the observation that GPECs undergo EMT like changes *in vitro* which generates metastable cells that express markers of both epithelia (CK-18) and mesenchyme (vimentin). Although, earlier study on human PECs do not mention of any EMT like changes, their report that clonally expanded $CD24^+$ $CD133^+$ cells exhibit uniform co-expression of cytokeratin and vimentin is interesting as this may intuitively point out that these cells are resultant of EMT. Parietal epithelial cells in the renal glomeruli are metanephric mesenchyme derived [10]; hence, any regression of these cells to embryonic phenotype should ideally include the conversion of terminally differentiated epithelial cells to a metanephric mesenchymal phenotype, preferably through EMT. Transcript analysis by qRT-PCR demonstrate that consistent with their metastability, these cells exhibit heterogeneous expression of metanephric mesenchymal (Pax-2, WT-1, Eya-1, Six-1, GDNF) as well as uteric bud (Hoxb-7,

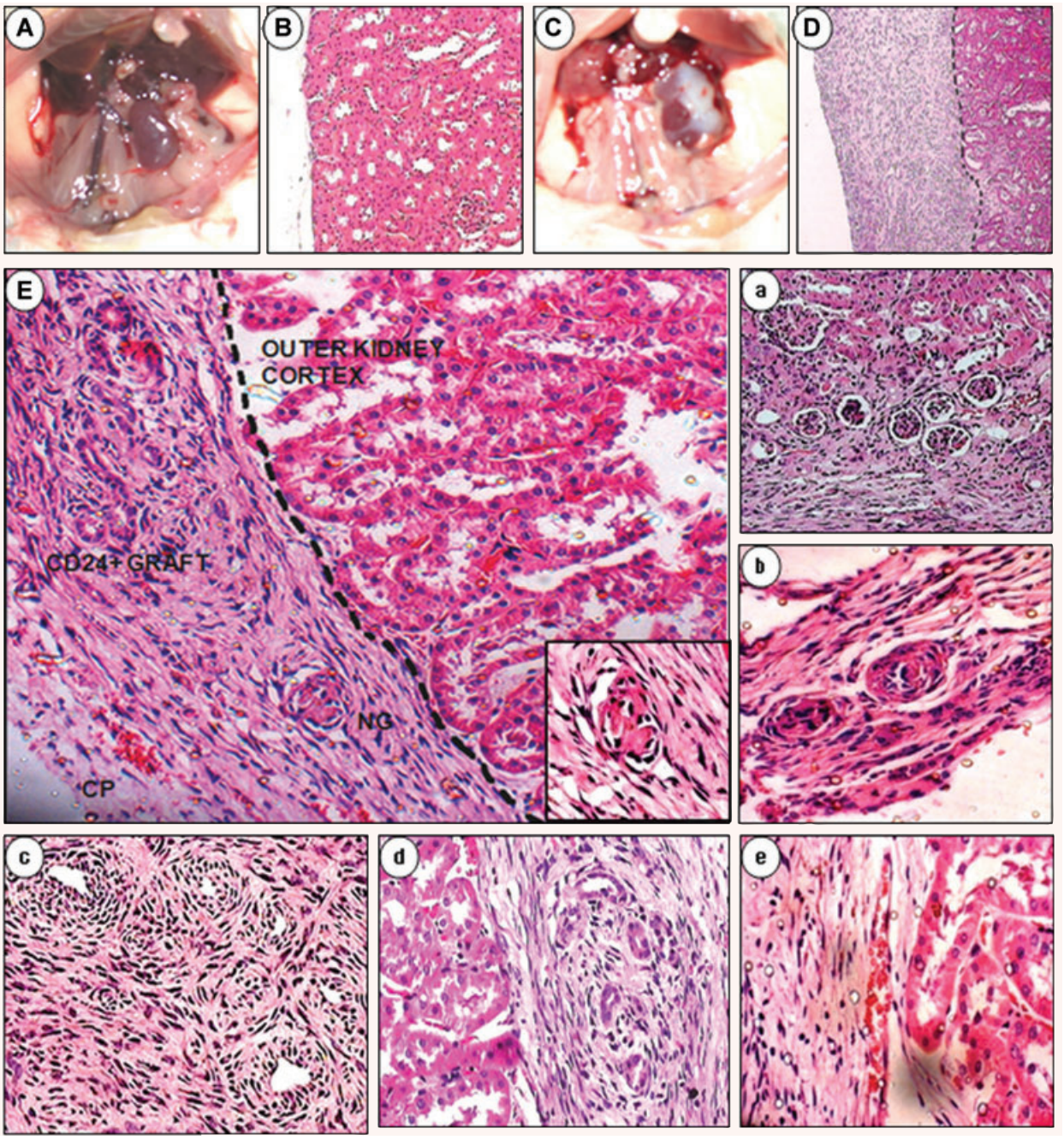

Fig. 7 $CD44^+$ $CD24^+$ cells exhibit *in vivo* renal commitment when grafted under the renal capsule of contra-lateral kidney of unilateral nephrectomized mice. $CD44^+$ $CD24^+$ cells were grafted under the left kidney capsule of normal mice. One week after implantation, right kidney was nephrectomized. Grafts were harvested 2 weeks after nephrectomy. Photographs showing contra-lateral kidney of unilateral nephrectomized mice-control kidney (without graft) (**A**) and test kidney (with graft) (**B**). Haematoxylin and eosin stained section of the control kidney (without graft) (**C**) and test kidney (with graft) (**D**). Note the thick layer of cellular graft under the renal capsule in the test kidney, which is absent in the control kidney. (Magnification = 100×). High magnification view of the graft sections showing neo-glomeruli like structures, vascularization (erythrocytes could be seen suggesting blood flow to the graft tissue) after 14 days of implantation (**E**). The dashed line separates the graft from the host. (Magnification = 200×). Grafts contained immature glomerular like structures (**E**.**a**, **b**), ducts (**E**.**c**, **d**) and vasculature with RBCs (**E**.**e**). The results are representative of five separate grafts.
Abbreviations: CP, capillary; NG, neo-glomeruli; RBC, red blood cells

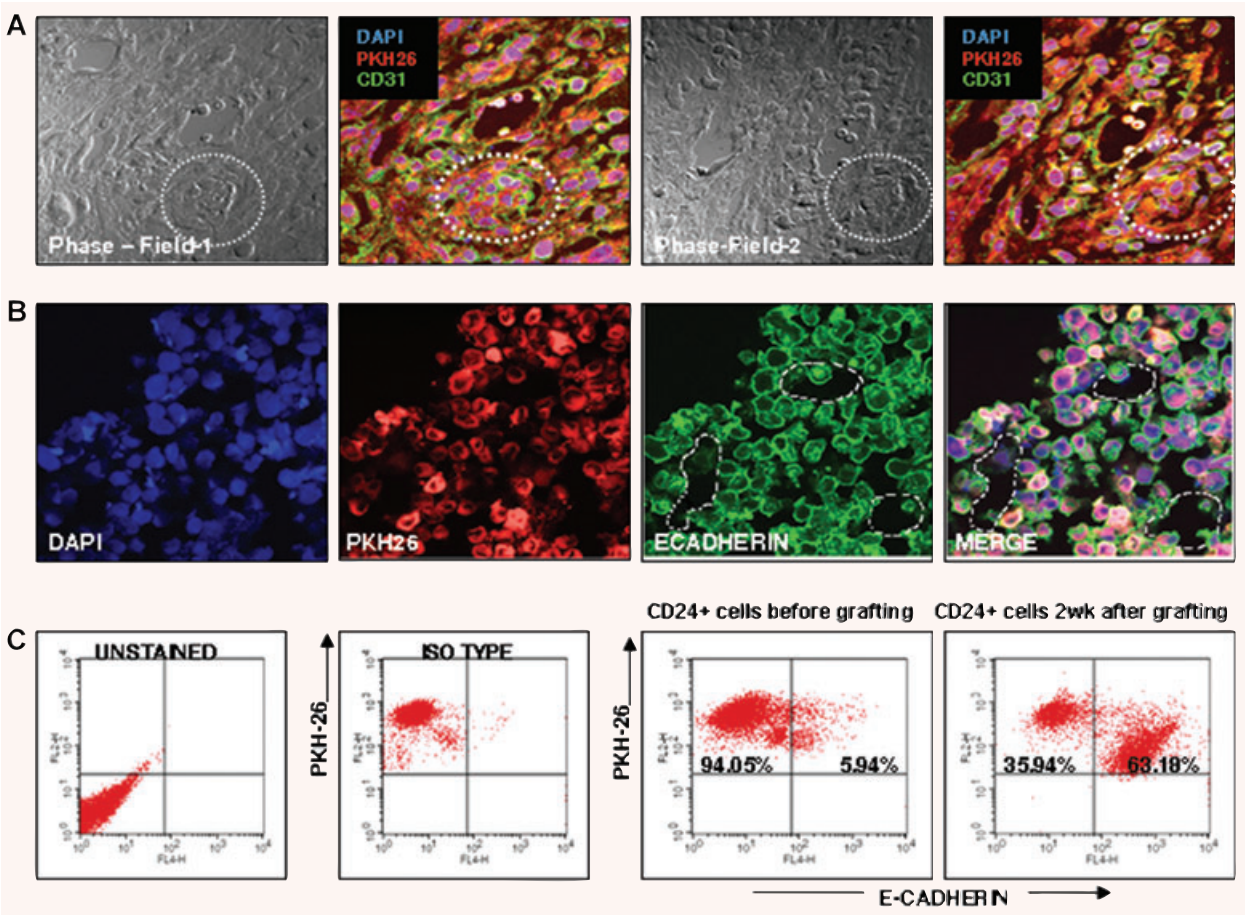

Fig. 8 PKH-26 labelled grafted CD44$^+$ CD24$^+$ cells show expression of adult kidney markers: representative confocal micrographs of cryostat sections of PKH-26 labelled CD44$^+$ CD24$^+$ grafts show neo-glomerular like structures co-expressing PKH26 with PECAM (CD31) (**A**). Epithelialization of the grafted cells was evident by the co-expression of PKH-26 with E-Cadherin (**B**). Flow cytometry analysis of the percentage of PKH 26 cells that underwent epithelial differentiation represented by E-Cadherin expression (63.18 ± 5%) (**C**).

C-Ret, K-Cadherin) genes, indicating that these cells might be bipotent renal progenitors. Taken together, our results suggest that GPECs have undergone partial EMT to generate bipotent progenitor cells. Emerging evidence suggests direct correlation between EMT and stemness [38]. In order to confirm that acquisition of progenitor markers by GPECs was EMT driven, we carried out PGE2 mediated EMT blocking experiments. Low transcript abundance was observed for most progenitor markers as well as Wnt genes, when EMT was blocked. Further, we observed that on EMT arrest; the rapid proliferative potential of GPECs was compromised, suggesting that EMT imparts survival and proliferative potential to the terminally differentiated GPECs. Despite the fact that EMT process in our culture system was spontaneous, possibly contributed by a number of growth factors, and there by blocking EMT using PGE2 might be partial, we observe that our results reflect a direct link between EMT and acquired stemness. This inference was further confirmed when CD24$^+$ putative kidney progenitors were tested in nephron development assays. Injection of fluorescently tagged CD24$^+$ cells into embryonic kidney organ culture resulted in the integration of the cells to kidney primordia. Additionally, co-culturing of CD24$^+$ cells with E13.5 spinal cord resulted in the formation of EBs, which on extended culture in matrigel exhibited distinct events of tubulogenesis such as formation of cellular processes, development of branching multi-cellular cords and establishment of tubules with lumens [39]. These results provide more convincing evidence on the functional progenitor status of these cells. Next, to definitively prove that CD24$^+$ cells could exhibit *in vivo* renal commitment,

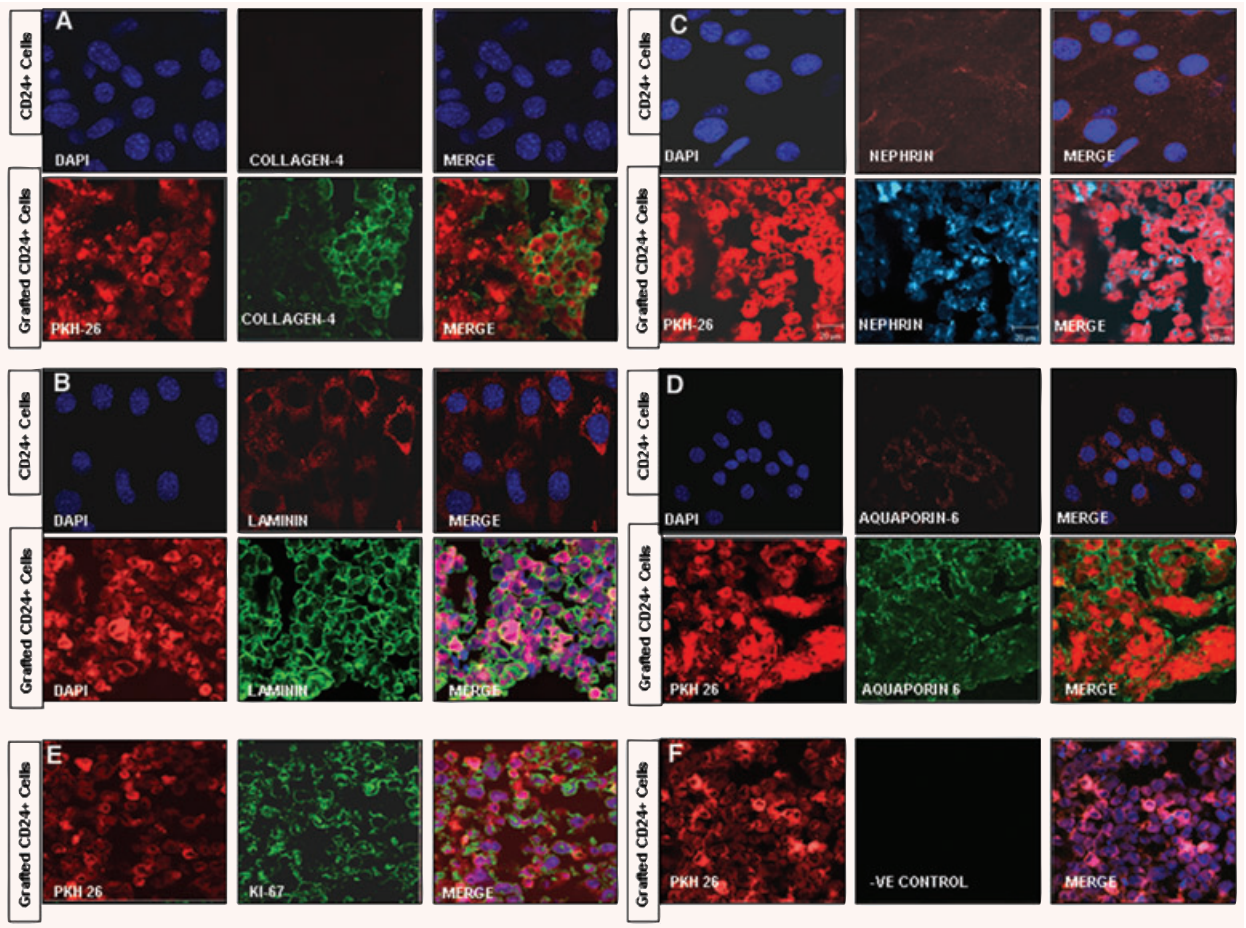

Fig. 9 Expression of kidney specific markers in the grafted cells: Expression of collagen-4 (**A**) and laminin (**B**) show that the grafted cells are surrounded by glomerular basement membranes indicating renal differentiation in these cells. Mature podocyte marker, Nephrin (**C**) and tubular water channel protein, Aquaporin-6 (**D**) were expressed by certain cells within the graft tissue. Note that non-grafted $CD24^+$ cells showed very low or no expression of the mature kidney markers. Grafted cells exhibited good proliferation potential *in vivo* as indicated by the expression of proliferative marker Ki-67 (**E**). Negative control (**F**) (Scale bar = 20 μm).

FACS sorted PKH-26 labelled $CD24^+$ cells were grafted under renal capsule of normal Swiss albino mice. One week after grafting, nephrectomy of the contra-lateral kidney was carried out. We observed that the grafted cells were capable of renal regeneration during compensatory renal growth and expressed markers associated with developing kidney. Co-expression of PKH-26 label with the assessed markers confirmed the donor origin of the graft. In summation, we show here that parietal epithelial cells of renal glomeruli, despite being highly committed could acquire properties of embryonic renal progenitors under the influence of EMT. Animal and human studies have often associated EMT to pathological conditions such as fibrosis and cancer [40]. In organs like kidney, EMT changes are described as initial response of the tissue towards injury which extrapolates by excessive ECM production leading to organ failure. Rapid fibrotic deposition however, is also reported to confer survival advantage to the tissue by preventing infection and mechanical damage [41].Understanding the cellular processes initiated during organ repair which ironically, at times, lead to organ failure, is very important for designing efficient therapeutic strategies and rescue renal pathology from this vicious cycle. Extrapolating our results to an *in vivo* scenario, we suggest that metastable cells with progenitor profile are generated through partial EMT by GPECs in response to glomerular injury. These metastable cells contribute to epithelial cell plasticity and reorganize the damaged tissue without losing all the epithelial characteristics [23]. Pathological situations like glomerular crescent formation and fibrosis may arise when these epithelial cells undergo total EMT, possibly

due to conditional aberrations in the regenerating milieu. However, in order to arrive at a conclusion, *in vivo* studies using animal models of renal injury need to be carried out to track cells undergoing EMT.

We ideate that the present study would improve our understanding on the plasticity exhibited by GPECs under EMT stimulation which would further our knowledge of its role in tissue homeostasis and disease progression and for possible intervention.

Acknowledgements

We thank the Director NCCS, Dr. G.C. Mishra for all the support. We also thank Dr. Avinash Pradhan, K.E.M. Hospital Pune, India, for expert comments on histological studies. We also thank Ashwini Atre for assistance with confocal microscopy and Swapnil Walke for FACS. S.G. and V.C. are supported by fellowship from the University Grants Commission (UGC), Government of India.

References

1. **Bahlmann FH, Fliser D**. The plasticity of progenitor cells–why is it of interest to the nephrologists? *Nephrol Dial Transplan*. 2009; 24: 2018–20.
2. **Oliver JA, Maarouf O, Cheema FH, *et al.*** The renal papilla is a niche for adult kidney stem cells. *J Clin Invest*. 2004; 114: 795–04.
3. **Bussolati B, Bruno S, Grange C, *et al.*** Isolation of renal progenitor cells from adult human kidney. *Am J Pathol*. 2005; 166: 545–55.
4. **da Silva Meirelles L, Chagastelles PC, Nardi NB.** Mesenchymal stem cells reside in virtually all post-natal organs and tissues. *J Cell Sci*. 2006; 119: 2204–13.
5. **Bruno S, Bussolati B, Grange C, *et al.*** Isolation and characterization of resident mesenchymal stem cells in human glomeruli. *Stem Cells Dev*. 2009; 18: 867–80.
6. **Paulsom R, Forbes SJ, Hodivala-Dilke K, *et al.*** Bone marrow contributes to renal parenchymal turnover and regeneration. *J Pathol*. 2001; 195: 229–35.
7. **Duffield S, Park KM, Hsiao LL, *et al.*** Restoration of tubular epithelial cells during repair of the postischemic kidney occurs independently of bone marrow-derived stem cells. *J Clin Invest*. 2005; 115: 1743–55.
8. **Anglani F, Forino M, Del Prete D, *et al.*** In search of adult renal stem cells. *J Cell Mol Med*. 2004; 8: 474–87.
9. **Anglani F, Ceol M, Mezzabotta F, *et al.*** The renal stem cell system in kidney repair and regeneration. *Front Biosci*. 2008; 13: 6395–05.
10. **Humphreys BD, Valerius MT, Kobayashi A, *et al.*** Intrinsic epithelial cells repair the kidney after injury. *Cell Stem Cell*. 2008; 2: 284–91.
11. **Johnson RJ**. The glomerular response to injury: progression or resolution? *Kidney Int*. 1994; 45: 1769–82.
12. **Ng YY, Fan JM, Mu W, *et al.*** Glomerular epithelial-myofibroblast transdifferentiation in the evolution of glomerular crescent formation. *Nephrol Dial Transpl*. 1999; 14: 2860−72.
13. **Appel D, Kershaw DB, Smeets B, *et al.*** Recruitment of podocytes from glomerular parietal epithelial cells. *J Am Soc Nephrol*. 2009; 20: 333–43.
14. **Sagrinati C, Netti GS, Mazzinghi B, *et al.*** Isolation and characterization of multipotent progenitor cells from the Bowman's capsule of adult human kidneys. *J Am Soc Nephrol*. 2006; 17: 2443–56.
15. **El-Nahas AM**. Plasticity of kidney cells: role in kidney remodeling and scarring. *Kidney Int*. 2003; 64: 1553–63.
16. **Bariety J, Hill GS, Mandet C, *et al.*** Glomerular epithelial-mesenchymal transdifferentiation in pauci-immune crescentic glomerulonephritis. *Nephrol Dial Transplant*. 2003; 18: 1777–84.
17. **Yee-Yung Nga, Yung-Ming Chenb, Tun-Jun Tsaib, *et al.*** Pentoxifylline inhibits transforming growth factor-beta signaling and renal fibrosis in experimental crescentic glomerulonephritis in rats. *Am J Nephrol*. 2009; 29: 43–53.
18. **Atre AN, Surve SV, Shouche YS, *et al.*** Association of small Rho GTPases and actin ring formation in epithelial cells during the invasion by Candida albicans. *FEMS Immunol Med Microbiol*. 2009; 55: 74–84.
19. **Dicker SE, Shirley DG**. Mechanism of compensatory renal hypertrophy. *J Physiol*. 1971; 219: 507–23.
20. **Bogdani M, Suenens K, Bock T.** Growth and functional maturation of beta-cells in implants of endocrine cells purified from prenatal porcine pancreas. *Diabetes*. 2005; 54: 3387–94.
21. **Ohse T, Pippin JW, Vaughan MR, *et al.*** Establishment of conditionally immortalized mouse glomerular parietal epithelial cells in culture. *J Am Soc Nephrol*. 2008; 19: 1879–90.
22. **Zeisberg M, Hanai J, Sugimoto H, *et al.*** BMP-7 counteracts TGF-beta1-induced epithelial-to-mesenchymal transition and reverses chronic renal injury. *Nat Med*. 2003; 9: 964–8.
23. **Kiefer JC, Neito A, Thiery JP.** Primer and interview: epithelial to mesenchymal transition. *Developmental Dynamics*. 2008; 237: 2769–74.
24. **Challen GA, Martinez G, Davis MJ, *et al.*** Identifying the molecular phenotype of renal progenitor cells. *J Am Soc Nephrol*. 2004; 15: 2344–57.
25. **Mazzinghi B, Ronconi E, Lazzeri E, *et al.*** Essential but differential role for CXCR4 and CXCR7 in the therapeutic homing of human renal progenitor cells. *J Exp Med*. 2008; 205: 479–90.
26. **Schedl A, Hastie N D.** Cross-talk in kidney development. *Curr Opin Genet Dev*. 2000; 10: 543–9.
27. **Schmidt-Ott KM, Barasch J**. WNT/beta-catenin signaling in nephron progenitors and their epithelial progeny. *Kidney Int*. 2008; 74: 1004–8.
28. **Merkel CE, Karner CM, Carroll TJ**. Molecular regulation of kidney development: is the answer blowing in the Wnt? *Pediatr Nephrol*. 2007; 22: 1825–38.
29. **Vainio SJ, Itäranta PV, Peräsaari JP, *et al.*** Wnts as kidney tubule inducing factors. *Int J Dev Biol*. 1999; 43: 419–23.
30. **Kispert A, Vainio S, McMahon AP**. Wnt-4 is a mesenchymal signal for epithelial transformation of metanephric mesenchyme in the developing kidney. *Development*. 1998; 125: 4225–34.
31. **Hardy KM, Garriock RJ, Yatskievych TA**. Non-canonical Wnt signaling through Wnt5a/b and a novel Wnt11 gene, Wnt11b, regulates cell migration during avian gastrulation. *Dev Biol*. 2008; 320: 391–01.
32. **Eger A, Stockinger A, Park J, *et al.*** beta-Catenin and TGFbeta signalling cooperate to maintain a mesenchymal phenotype after FosER-induced epithelial to mesenchymal transition. *Oncogene*. 2004; 23: 2672–80.

33. **Zhang A, Wang MH, Dong Z, *et al*.** Prostaglandin E2 is a potent inhibitor of epithelial-to-mesenchymal transition: interaction with hepatocyte growth factor. *Am J Physiol Renal Physiol.* 2006; 291: 1323–31.
34. **Kim D, Dressler GR**. Nephrogenic factors promote differentiation of mouse embryonic stem cells into renal epithelia. *J Am Soc Nephrol.* 2005; 16: 3527–34.
35. **Herzlinger D, Qiao J, Cohen D, *et al.*** Induction of kidney epithelial morphogenesis by cells expressing Wnt-1. *Dev Biol.* 1994; 166: 815–8.
36. **St John PL, Abrahamson DR**. Glomerular endothelial cells and podocytes jointly synthesize laminin-1 and -11 chains. *Kidney Int.* 2001; 60: 1037–46.
37. **Yasui M, Kwon TH, Knepper MA, *et al.*** Aquaporin-6: an intracellular vesicle water channel protein in renal epithelia *Proc Natl Acad Sci USA.* 1999; 96: 5808–13.
38. **Mani SA, Guo W, Liao MJ, *et al.*** The epithelial-mesenchymal transition generates cells with properties of stem cells. *Cell.* 2008; 133: 704–15.
39. **Sakurai H, Barros EJ, Tsukamoto T, *et al.*** An *in vitro* tubulogenesis system using cell lines derived from the embryonic kidney shows dependence on multiple soluble growth factors. *Proc Natl Acad Sci USA.* 1997; 94: 6279–84.
40. **Radisky DC, Kenny PA, Bissell MJ**. Fibrosis and cancer: do myofibroblasts come also from epithelial cells via EMT. *J Cell Biochem.* 2007; 101: 830–9.
41. **Romagnani P, Kalluri R**. Possible mechanisms of kidney repair. *Fibrogenesis Tissue Repair.* 2009; 2: 3.